

Looking to diversify suppliers for MRI contrast agents?

Two cost-effective generic options available. Now you have a choice.

DISCOVER GENERIC  
CONTRAST AGENTS

 FRESENIUS  
KABI

# AJNR

## Theoretic Basis and Technical Implementations of CT Perfusion in Acute Ischemic Stroke, Part 2: Technical Implementations

A.A. Konstas, G.V. Goldmakher, T.-Y. Lee and M.H. Lev

This information is current as  
of January 25, 2025.

*AJNR Am J Neuroradiol* 2009, 30 (5) 885-892

doi: <https://doi.org/10.3174/ajnr.A1492>

<http://www.ajnr.org/content/30/5/885>

# Theoretic Basis and Technical Implementations of CT Perfusion in Acute Ischemic Stroke, Part 2: Technical Implementations

## PHYSICS REVIEW

A.A. Konstas  
G.V. Goldmakher  
T.-Y. Lee  
M.H. Lev

**SUMMARY:** CT perfusion (CTP) is a functional imaging technique that provides important information about capillary-level hemodynamics of the brain parenchyma and is a natural complement to the strengths of unenhanced CT and CT angiography in the evaluation of acute stroke, vasospasm, and other neurovascular disorders. CTP is critical in determining the extent of irreversibly infarcted brain tissue (infarct “core”) and the severely ischemic but potentially salvageable tissue (“penumbra”). This is achieved by generating parametric maps of cerebral blood flow, cerebral blood volume, and mean transit time.

Part 1 of this review established the clinical context of CT perfusion (CTP).<sup>1</sup> Next, a discussion followed on CTP map construction using the maximum slope method and the 2 main deconvolution techniques, Fourier transformation and singular value decomposition (SVD) (the latter being the most commonly used numeric method in CTP). Part 2 discusses the “pearls and pitfalls” of CTP map 1) acquisition, 2) postprocessing, and 3) image interpretation. Issues including radiation dose-reduction strategies, methods of correcting arterial input function (AIF) delay, the effect of the laterality of AIF choice, vascular pixel elimination, the importance of correct cerebral blood flow (CBF) and cerebral blood volume (CBV) threshold selection, and the selection of appropriate perfusion parameters for correct estimation of penumbra are addressed. The review highlights the need for validation and standardization of important CTP parameters to improve patient outcomes and design future randomized clinical trials that will provide evidence for the importance of the core/penumbra “mismatch” in patient triage for recanalization therapies beyond the current 3-hour therapeutic window for intravenous thrombolysis.

### Technical Implementations

#### CTP Acquisition

At a recent meeting of stroke radiologists, neurologists, emergency physicians, National Institutes of Health (NIH) administrators, and industry leaders in Washington, DC, sponsored by the NIH and the American Society of Neuroradiology, both technical and clinical issues regarding advanced acute stroke imaging were discussed. Expert consensus regarding standardized CTP and MR perfusion (MRP) acquisition was achieved, published simultaneously as a position paper in *American Journal of Neuroradiology* and *Stroke*.<sup>2,3</sup> The baseline CT study should have 3 components: unenhanced CT, vertex-to-arch CT angiography (CTA), and dynamic first-pass CTP.<sup>4</sup> Addition of cardiac multidetector row CT (MDCT) for the detection of possible left atrial appendage thrombus is optional but may gain in popularity because cardioembolic

strokes comprise about one third of all ischemic strokes (and their incidence appears to be increasing as stent placement/endarterectomy for primary stroke prevention of carotid embolic stroke becomes more common place).<sup>5</sup> Ruling out a cardiac source may have important consequences for patient management. A recent study reported 80% specificity, 73% sensitivity, and 92% negative predictive value for cardiac MDCT compared with more invasive transesophageal echocardiography.<sup>6</sup> Another recent study reported a positive predictive value of 99% and a negative predictive value of 96%,<sup>7</sup> making cardiac MDCT an appealing component for an integrated neurovascular protocol. Sample CTP scanning parameters based on the general consensus of the meeting and our institutional protocols by using a 64-section volume MDCT (LightSpeed; GE Healthcare, Waukesha, Wis) are shown in Tables 1 and 2.

**Contrast Administration.** For CTP, A contrast bolus of 35–45 mL is administered via power injector at a rate of 7 mL/s, with a saline “chaser” of 20–40 mL at the same injection rate. The contrast used should typically be a high concentration, ideally 350–370 g/dL of iodine, to create the greatest peak enhancement and hence the optimal signal-intensity-to-noise ratio for CTP map calculation.

**Image Acquisition.** Imaging in cine mode (CT table stationary) begins a few seconds after injection. In the past, protocols were designed to acquire 1 image per second for 45 seconds,<sup>2,8,9</sup> principally to minimize radiation dose. However, this relatively short imaging time risks obtaining an incomplete concentration of tissue,  $C_{tissue}(t)$ , curve in patients with poor cardiac output, atrial fibrillation, and proximal internal carotid artery occlusion or hairline lumen. Additionally, measurements of blood-brain barrier (BBB) permeability may be possible from time-attenuation curves (TDC), but this also requires longer acquisition times.

Due to these considerations, acquisitions of at least 60 and typically 75–90 seconds have become standard. A potential problem with this, however, is that extending the scanning time can increase the patient’s radiation exposure. One solution is to use an acquisition that consists of 2 or even 3 phases (the latter if permeability imaging is required). In the first phase, images can be acquired once a second for 40 seconds. In the second phase, images can be acquired once every 2–3 seconds for an additional 35–45 seconds (total of at least 75 seconds). If permeability measurements are required, a third phase, in which images are acquired every 10–15 seconds for

From the Department of Radiology (A.A.K., G.V.G., M.H.L.), Massachusetts General Hospital, Boston, Mass; and Imaging Research Laboratories (T.-Y.L.), Robarts Research Institute, London, Ontario, Canada.

Please address correspondence to Angelos A. Konstas, MD, Department of Radiology, Massachusetts General Hospital, 55 Fruit St, Boston, MA 02114; e-mail: akonstas@partners.org

DOI 10.3174/ajnr.A1492

**Table 1: Sample acute stroke protocol for 64-section MDCT scanner: NCCT, vertex-to-arch CTA with cardiac component, and standard cine CTP**

	Location	Section Thickness (mm)	Image Spacing (mm)	Pitch	kV	mA	Gantry Rotation Time (s)	Contrast Administration
NCCT	C1 to vertex	5	5	0.531:1	120	250	0.7	
CTA	Vertex to 1 cm below carina	1.25	0.625	0.516:1	120	420	0.5	4 mL/s; volume, 40-mL contrast
Cardiac	Carina to just below diaphragm	0.625	0.625	1:1	120	420	0.35	Repeat after 45-second delay
Cine CTP	Selected by neuroradiologist	4-cm slab	N/A	N/A	80	200	1	7 mL/s; volume, 35 mL

**Note:**—NCCT indicates noncontrast CT; N/A, not applicable; MDCT, multidetector row CT; CTA, CT angiography; CTP, CT perfusion.

**Table 2: Sample acute stroke protocol for 64-section MDCT scanner: NCCT, vertex-to-arch CTA without cardiac component, and shuttle-mode CTP**

	Location	Section Thickness (mm)	Image Spacing (mm)	Pitch	kV	mA	Gantry Rotation Time (s)	Contrast Administration
NCCT	C1 to vertex	5	5	0.531:1	120	250	0.7	
CTA	Vertex to 1 cm below carina	1.25	0.625	0.516:1	120	200–660	0.5	4 mL/s; volume, 60-mL contrast
Shuttle-mode CTP	Selected by neuroradiologist	8-cm slab	N/A	N/A	80	500	0.4	7 mL/s; volume, 45 mL

an additional 2 minutes, can also be added. Because late changes in contrast opacification occur less rapidly, late images can be obtained at a lower frequency than that required for first-pass images.<sup>10</sup>

To date, there is limited experience with quantification of the permeability of the BBB in acute stroke; most studies have assessed the vascular permeability of tumors.<sup>11</sup> The severity of BBB disruption has, however, been shown to correlate with outcome in ischemic stroke, and more routine incorporation of permeability measurements in the near future is possible.<sup>11</sup> Similarly, a recent study suggested the potential of permeability MR imaging to identify patients with acute ischemic stroke at higher risk for hemorrhagic transformation.<sup>12</sup> Existing deconvolution techniques can be extended to enable quantification of BBB permeability.<sup>13,14</sup> Overall, the approach outlined above allows good temporal resolution at the start of scanning, when sampling the TDC frequently is more important for good curve fitting but does not truncate a TDC that has some delay in washout due to delayed contrast delivery. At the same time, less frequent sampling ensures that overall radiation exposure is not significantly increased.

**Image-Acquisition Parameters.** The CTP imaging protocol has always been performed at 80 kV, rather than the more conventional 120–140 kV. Theoretically, given a constant milliamper-second (typically 200 mAs), this kilovolt setting would not only reduce the administered radiation dose to the patient but would also increase the conspicuity of intravenous contrast due, in part, to greater importance of the photoelectric effect for 80-kV photons, which are closer to the “k-edge” of iodine.<sup>15</sup>

**Z-Direction Coverage and Section Thickness.** The volume of brain tissue included in a first-pass cine CTP study is constrained in the craniocaudal direction by the width of the CT detector. Hence, the z-axis coverage of each acquisition depends on the manufacturer and generation of the CT scanner. This limitation arises from the routine rapid early acquisition rate of 1 image per second, which does not allow sufficient time for tabletop movement. The detector configuration can be varied so that a number of different section thicknesses can be obtained simultaneously. For example, with a 16-de-

tector row scanner, a 2-cm slab is obtained, consisting of either two 10-mm or four 5-mm-thick sections.<sup>8,9,16</sup> With a 64-detector row scanner, a 4-cm slab can be acquired with each injection.

The maximum degree of vertical coverage could potentially be doubled for each bolus by using a “shuttle-mode” technique, in which the scanner table moves back and forth, switching between 2 different cine views, albeit at a reduced temporal resolution of data acquisition.<sup>17</sup> Alternatively, 2 boluses can be used to acquire 2 slabs of CTP data at different levels, doubling the overall coverage,<sup>18</sup> but—unlike shuttle mode—requiring twice the contrast and twice the radiation dose.

Coverage volume will continue to increase with enlarging detector arrays and improved technology. Cutting edge scanners with 320 detector rows offer the possibility of 16-cm coverage without the decreased temporal resolution required with the shuttle-mode technique. However, the optimum temporal resolution for accurate measurement of CBF, CBV, and mean transit time (MTT) is not yet resolved. Wintermark et al (2004)<sup>19</sup> studied the effect of changing the sampling interval to 0.5, 1, 2, 3, 4, 5, and 6 seconds, respectively, on the derived CBF, CBV, and MTT parameters, by progressively skipping more images from the original image sequence at 0.5-second intervals. If 10% deviations from the reference CBF, CBV, and MTT values derived at a 1-second image interval are allowed, the image interval could be increased to 2–3 seconds for both normal and ischemic tissue without substantial variance in quantification. Thus, the axial shuttle technique with a sampling interval of ~3 seconds may be a relatively straightforward and inexpensive method to increase z-direction coverage from 4 to 8 cm for 64-section scanners.

**Radiation Dose-Reduction Strategies.** Neuroradiologists are familiar with factors that affect patient dose such as pitch, milliamper-second, kilovoltage peak (kV[p]), and collimation, but there are additional ways to further reduce radiation exposure. The combination of low kilovoltage peak (80 kV[p]) with low milliamper-second (typically 200 mAs) has already been noted and is an accepted strategy for dose reduction.<sup>9,20,21</sup>

(Tube current is directly proportional to dose but at a cost of increased noise, which is increased by  $1/\sqrt{\text{mA}}$ ).

Another method of dose reduction is by decreasing the image frequency of acquisition from the CTP first-pass data. As discussed above, Wintermark et al (2004)<sup>19</sup> calculated maps for temporal sampling intervals of 0.5, 1, 2, 3, 4, 5, and 6 seconds in patients with ischemic stroke. Sampling intervals up to 3 seconds in protocols using a 40-mL bolus did not demonstrate a significant over- or underestimation estimation of CBF, CBV, or MTT. CBF and CBV were overestimated and MTT was underestimated only when sampling intervals were beyond 4 seconds. These results suggest that radiation dose can be reduced by up to two thirds during the first phase without altering the quantitative accuracy of CTP (such as is achieved in shuttle-mode acquisition). The effective radiation dose varied between 0.852 and 1.867 mSv, depending on the protocol. The cine mode with two 40-mL boluses and the shuttle-mode technique with one 60-mL bolus had the lowest doses.

To put the above dose ranges into perspective, an axially acquired head CT on a standard 64-section volume CT scanner typically has a 3.2-mSv effective radiation dose. For comparison, the background radiation for a person living in Boston for a year is approximately 3 mSv or about that of 1 standard head CT. The radiation from a 4-cm coverage, 1 image/second, single-bolus standard CTP performed at our institution without shuttle mode is approximately 3.7 mSv or slightly more than that of 1 standard head CT. Shuttle mode gives twice the coverage at substantially lower total dose, because we are imaging about once every 3 seconds for 75–90 seconds.

### Postprocessing

**General Principles.** Following CTP data acquisition, source images are generally transferred to a freestanding workstation for processing into parametric maps. There are multiple manufacturers of software packages capable of such processing. Although some of these software packages process maps on the basis of the maximum slope method, increasingly deconvolution-based software is being used for the reasons outlined earlier. Postprocessing can be manual, semiautomated, or fully automated. Inputs required for CTP map calculation include the AIF and the venous output function (VOF). Some software packages also incorporate image-processing algorithms that automatically identify a range of tissue and vascular structures, a process known as “image segmentation.” Noncerebral tissue, such as sulci, arteries, and veins, is readily removed from CTP maps by image segmentation, by using thresholds based on attenuation measurements. Gray matter typically measures 30–40 HU and white matter, 20–30 HU; removal of pixels  $<0$  HU or  $>60$ –80 HU effectively eliminates bone, fat, and air from unenhanced CT images.<sup>22</sup> Alternatively, thresholds can be based on the actual parametric map values.

The AIF can be selected by identifying a subset of pixels within a larger region of interest placed by the operator to encompass a candidate artery. It is important to try to select a vessel that is orthogonal to the imaging plane to minimize volume averaging. A venous region of interest is next selected to serve as the venous output function. The purpose of the

VOF is to serve as a reference for normalization of the quantitative CTP parameter values, relative to a nonvolume averaged maximum intravascular contrast measurement. Because veins (particularly the posterior superior sagittal sinus) are typically larger than arteries, the venous TDC is not as subject to partial volume averaging as is the arterial TDC. As noted, accurate CTP quantification requires selection of an appropriate venous outflow region of interest, with sufficient “wash in” and washout of contrast to serve as a normalization or scaling factor for the CTP parameter values.<sup>23</sup> By comparing the areas of the venous and arterial TDCs, one can correct for the partial volume averaging of the arterial TDC.<sup>14</sup> Processing of raw data based on these selections yields quantitative parametric maps of CBV, CBF, and MTT from the principles outlined previously in the section on CT perfusion theory and modeling.<sup>1</sup>

Peripheral blood vessels and perforating arteries should be excluded from CTP maps because they may mimic areas of falsely high perfusion within brain tissue.<sup>22</sup> Kudo et al (2003)<sup>24</sup> evaluated the efficacy of vascular pixel elimination in CTP imaging in comparison with positron-emission tomography (PET). Any pixel with a higher CBV value than a threshold of 8 mL/min was marked and eliminated from the CBF calculation. The correlation of CT-CBF and PET-CBF measurements was significantly improved when pixels with CBV values above that threshold were eliminated. Vascular pixel elimination appears to be especially useful when the quantitative CBF values of cortical gray matter are of concern. This method eliminates the leptomeningeal vessels that are otherwise almost always present in the subarachnoid space sulci and hence prevents overestimation of CBF.

**Methods of Correcting for Delay and Dispersion of the AIF.** Calculation of CBF requires knowledge of the AIF, which in practice, one estimates from a major artery, assuming that it represents the exact and only input to the tissue voxel of interest, with neither delay nor dispersion. There are several clinical situations, however, in which the AIF TDC will lag, and the tissue TDC will lag behind the AIF curve (“delay”; Fig 1). AIF delay can be due to extracranial causes (atrial fibrillation, severe carotid stenosis, poor left ventricular ejection fraction) or to intracranial causes (proximal intracranial obstructive thrombus with poor collaterals). Moreover, in such cases, the contrast bolus forming the AIF can spread out over multiple pathways proximal to the tissue region of interest (“dispersion”). Delay and dispersion can result in grossly underestimated CBF and overestimated MTT.<sup>25–27</sup>

Several approaches have been used to minimize the effects of delay and dispersion in SVD methods. Of note, although Fourier techniques are insensitive to delay, they are very sensitive to noise and thus unsuitable for CBF calculations. Wu et al (2003)<sup>27</sup> reported a tracer-arrival timing-insensitive technique using SVD with a block circulant decomposition matrix. The investigators removed the causality assumption built into SVD (ie, that the tissue-of-interest signal intensity cannot arrive before the AIF). This is certainly possible if the AIF is measured from a diseased vessel. Therefore, the calculated  $R(t)$  would be shifted by a time delay, but if causality is assumed,  $R(t)$  cannot properly be estimated by the deconvolving equation 13. By using circular instead of linear deconvolution (standard SVD), however, the calculated  $R(t)$  can now be represented, with  $R(t)$  circularly shifted by the time delay. In other

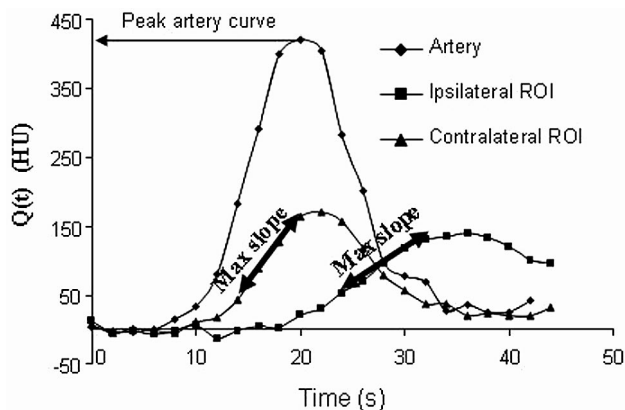


**Fig 1.** The maximum slope method. CBF can be calculated from the ratio of the maximum slope (Max Slope) of  $Q(t)$  to the maximum arterial concentration. The higher maximum slope in the contralateral region of interest (ROI) (ie, the region of interest without stroke) will give a higher CBF than that for the ipsilateral region of interest, for which the CBF will be reduced.

words, circular deconvolution avoids the time aliasing of linear deconvolution.

Block circulant deconvolution was demonstrated to be insensitive to tracer arrival-time differences with both numeric simulations and clinically acquired data.<sup>28</sup> Most important, circular deconvolution performed comparably with standard SVD when there were no tracer arrival-time differences. A recent study in patients with large territorial infarcts confirmed that circular deconvolution outperformed linear deconvolution.<sup>28</sup> Moreover, imaging acquisition intervals of  $>2$  seconds were used, lowering radiation exposure without decreasing the signal-intensity-to-noise ratio.<sup>28</sup> Members of the Acute Stroke Imaging Standardization (ASIST) group in Japan are currently working with analysis software vendors to implement block circulant deconvolution into their commercial systems (<http://plaza.umin.ac.jp>).

Another approach to delay correction is to use a local AIF estimated from a smaller vessel closer to the tissue of interest. Initial attempts to measure a local AIF were problematic due to partial volume effects.<sup>29,30</sup> More recently, automated local AIF selection algorithms for MRP have yielded promising results,<sup>31,32</sup> though experience with CTP is lacking. Alternatively, independent component analysis can be used as a tool to define the local AIF. Independent component analysis can be used to identify spatially independent patterns and is based on the assumption that signals of interest can be decomposed into a linear combination of statistically independent components.<sup>33</sup> Calamante et al (2004)<sup>33</sup> have provided a comprehensive description of this methodology and have compared it with the conventional approach of global AIF in MRP imaging data from patients with various cerebrovascular abnormalities. The independent component analysis approach produced higher CBF and shorter MTT values, compared with the global AIF method, in areas of distorted AIFs, suggesting that the effects of delay and dispersion are minimized. Moreover, independent component analysis demonstrated improved signal-to-noise ratio due to its “denoising” capabilities.

Yet another approach is to determine the relative time difference between the AIF( $t$ ) and  $C_{tissue}(t)$  TDCs by curve-fitting. Ibaraki et al (2005)<sup>34</sup> used a pixel-by-pixel least squares fitting as an initial preparatory step before SVD deconvolu-

tion. Only the data preceding the AIF( $t$ ) peak were fitted to determine delay, because the “tail” portion of the data reflects the tissue passage of contrast, rather than the tracer-arrival timing. Still another approach is to incorporate the estimation of delay directly into the deconvolution algorithm. Both these latter approaches are simpler to implement than circular deconvolution and independent component analysis. These delay-correction techniques have successfully corrected the underestimation of CBF inherent with SVD deconvolution. Incorporation and standardization of robust AIF delay correction into commercially available CTP software are needed to ensure the reproducibility and reliability of CTP map calculation (Fig 2). To date, only a very small number of vendors have introduced such postprocessing software, though as previously noted, this is a rapidly changing field with frequent new releases by manufacturers (see *ASIST-Japan Website*: <http://plaza.umin.ac.jp>).

Delay correction is especially critical when intracranial or extracranial causes of circulatory derangement are present. A recent study identified a very small percentage of cases in which the final infarct size following thrombolysis appeared smaller than that predicted by the admission core CBV lesion size calculated by using older generation delay-sensitive software.<sup>35</sup> Perfusion maps were recalculated by using a newer commercially available delay-insensitive algorithm. Only 2 of the initial 11 reversible CBV lesions were found to be truly reversible when recalculated by using the newest delay-insensitive software, suggesting that true reversibility of the CBV infarct core is exceedingly rare. Of note, the delay-sensitive software calculated CBV from MTT and CBF according to the central volume principle ( $CBV = MTT \times CBF$ ); both MTT and CBF were, in turn, derived by using a deconvolution algorithm without any of the delay-correction strategies discussed above. Hence, most cases of apparent CT-CBV reversibility, which is rare, are actually pseudoreversible and may be attributed to technical issues associated with lack of delay correction in CTP map postprocessing.

**Implications of Laterality of AIF Choice.** No general consensus has been reached as to whether the AIF should be chosen ipsi- or contralateral to the affected hemisphere, and to date, to our knowledge, few studies have addressed this controversy, though the use of standardized delay-corrected postprocessing software in the future should render this point moot. Some have argued that the assumptions underlying most perfusion models are best met by choosing 2 AIFs—a left-sided one for the left hemisphere and a right-sided one for the right hemisphere.

Sanelli et al (2004)<sup>23</sup> constructed CTP maps at the infarct core of 3 patients and reported that CBF, CBV, and MTT values were independent of the location and size of regions of interest selected for the AIF. Choosing a large proximal intracranial artery versus a smaller distal artery ipsilateral or contralateral to the infarct did not affect the resulting quantitative perfusion values. A more recent study of 18 patients with acute stroke has also reported that infarct core and penumbral CBV and CBF values were significantly correlated between ipsi- and contralateral AIF selection.<sup>36</sup> The correlations between infarct core MTT values obtained with different AIFs were lower than those obtained for CBF and CBV, though not significantly; there was no significant correlation of the MTT values in the

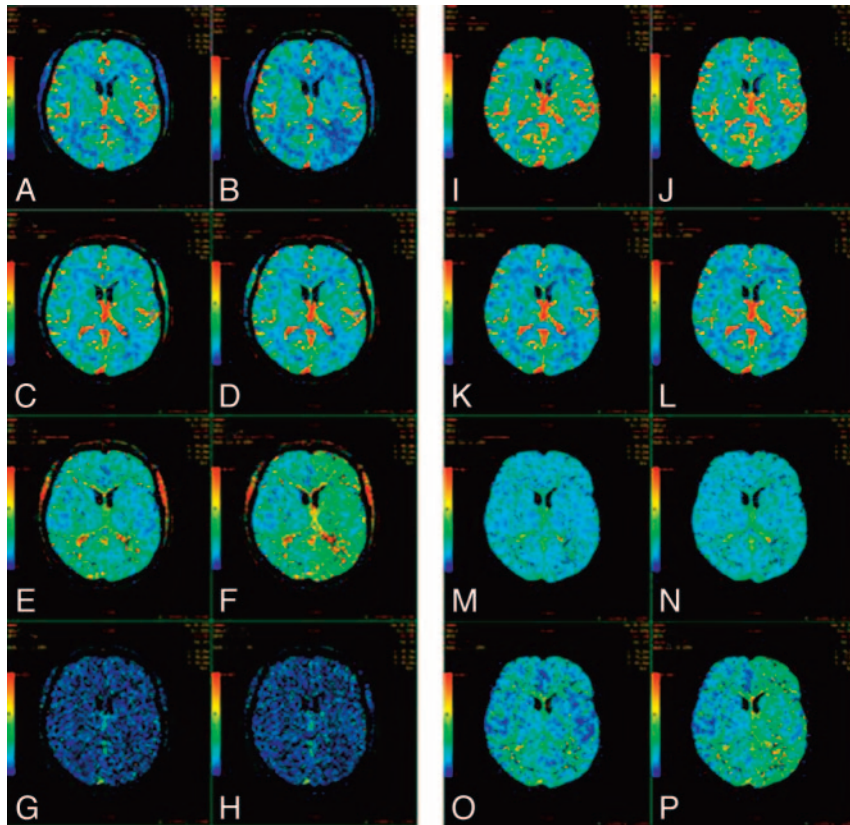


**Fig 2.** A–H, CTP maps calculated by using a delay-sensitive deconvolution algorithm that is affected by the delay ( $T_o$ ) between arterial input and tissue curves. To simulate a range of  $T_o$ , we processed the dynamic images of a single section from a CTP study on a patient with brain tumor such that time-versus-enhancement curves from the entire left hemisphere were shifted forward in time by 2 seconds relative to the right hemisphere. The original and time-shifted CTP studies were then processed by Perfusion 3 (GE Healthcare) by using the same arterial input curve and venous curve from the right hemisphere. A and B, CBF maps for the original and the  $T_o = 2$  second study. C and D, The corresponding CBV maps. E and F, The corresponding MTT maps. G and H, The corresponding  $T_o$  maps. As  $T_o$  increases, CBF decreases and MTT increases while CBV remains unchanged. The deconvolution algorithm is not able to estimate  $T_o$ . I–P, CTP maps calculated by using a delay-insensitive deconvolution algorithm that is unaffected by the  $T_o$  between arterial input and tissue curves. The original and time-shifted CTP studies of I–P are processed in the same way as A–H except that a delay-insensitive deconvolution algorithm (Perfusion 4, GE Healthcare) is used instead. I and J, The CBF maps for the original and  $T_o = 2$  second study. K and L, The corresponding CBV maps. M and N, The corresponding MTT maps. O and P, The corresponding  $T_o$  maps. As  $T_o$  increases, CBF and CBV remain relatively unchanged and MTT increases slightly. The deconvolution algorithm is able to detect an increase in  $T_o$ , but the estimate of  $T_o$  is not accurate.

penumbra. Of note, in both studies above, AIF with substantial delays due to severe stenosis or atrial fibrillation were not specifically studied.

Unpublished data from CTP maps of 14 patients with acute stroke at our institution, processed with delay-insensitive software, also suggest that the laterality of the AIF region of interest does not significantly influence the CBV, CBF, and MTT values in the infarct core. AIF selection by using delay-corrected deconvolution based on CTP software appears to be less sensitive to laterality compared with the use of standard available MRP software, which typically is not delay-corrected.<sup>37</sup> The inherent difficulties of choosing an optimal AIF from gradient-echo MR imaging source images may also add to the imprecision in reliably measuring perfusion parameters with MRP.<sup>29,38</sup> Moreover, because to date, CTP is an “on label” US Food and Drug Administration–approved use of iodinated CT contrast but MRP remains an “off label” indication for gadolinium-based agents, there has understandably been greater interest in developing CTP rather than MRP commercial software packages.

#### Fully Automated Processing of Stroke CTP Maps.

Recently released software-analysis packages can reliably and rapidly construct CTP maps fully automatically, resulting in true 1-mouse-click turnkey functionality. We preliminarily

assessed 1 such system, constructing CTP maps from 20 patients with acute stroke, first manually and then automatically (Perfusion 4; GE Healthcare). Gray and white matter regions of interest were sampled in normal tissue, and quantitative measurements of CBV, CBF, and MTT were made. Overall, there was very good agreement between the manually constructed and the automatically processed maps, with the exception of minimal disagreement in white matter CBF values. Automated processing of CTP maps has the potential to be of practical value for triage of patients with stroke in emergency settings because it is faster, easier, and likely as accurate as manual map construction.<sup>39</sup>

The precision of quantitative CTP values is directly linked to the reproducibility of the postprocessing procedure. Most commercially available CTP postprocessing software requires the operator to choose subjectively regions of interest and define parameters that are subsequently applied to the calculations that generate the CBV, CBF, and MTT maps. A recent study reported the variability of CTP data processed by different experienced technologists to be 31%, 30%, and 14% for CBV, CBF, and MTT, respectively.<sup>40</sup> The selection of AIF regions of interest, venous function regions of interest, and pre-enhancement intervals (another user-defined parameter describing the baseline of the TDC to be applied before con-

trast arrival) was very reproducible. The technologists differed significantly with respect to the selection of the post-enhancement interval (which is used to define such factors as recirculation). In this respect, fully automated processing of stroke CTP maps, as discussed above, could potentially increase both the precision and accuracy of CBF and CBV determination.

### **CTP Map Image Interpretation: Challenges and Limitations**

**CBF and CBV Thresholds.** An important role of advanced stroke imaging is to provide an assessment of ischemic tissue viability that transcends an arbitrary clock time.<sup>41-43</sup> Evidence suggests that the distinction between infarct core and penumbra can be achieved by applying thresholds to the CBF and CBV values.<sup>18,44</sup> Ischemic core has a matched decrease in both parameters, whereas the penumbra demonstrates a reduction in CBF with CBV that is maintained, or even elevated, relative to normal contralateral values. The maintained CBV in the penumbra can be attributed to dilation of precapillary arterioles and to engorgement of veins in response to decreased perfusion pressure.<sup>45</sup> Matched reduction of CBF and CBV in the ischemic core is thought to be due to the failure of autoregulation with severe hypoperfusion. To define the penumbra and ischemic core, thresholds must be selected for CBF and CBV.

With regard to these operationally defined thresholds for core and penumbra, though there is not yet consensus or high-level evidence, current expert opinion favors the use of relative rather than absolute CTP values, given the potential for variability in absolute quantification of CTP map parameters and the dependence of these values on an appropriate but often arbitrary VOF scaling factor.

In a pilot study of CTP thresholds for infarction, we found that a <50% reduction of CT-CBF in the penumbra has a high probability of region survival, whereas penumbra with a >66% reduction from baseline values has a high probability of infarction. No region with absolute CBV < 2.2 mL/100 g survived.<sup>4,46</sup> The latter is in close agreement with the CBV threshold of 2.0 mL/100 g selected by Wintermark et al to define core.<sup>18,47</sup> Because CBV and CBF have different baseline values in gray and white matter, however, (gray matter CBV ~ 4 mL/100 g/min, white matter CBV ~ 2 mL/100 g/min; and gray matter CBF ~ 40–60 mL/100 g/min, white matter CBF ~ 20–30 mL/100 g/min), it is critical that the contralateral regions of interest used for normalization have the same gray matter/white matter ratio as the ipsilateral ischemic region under study.

Despite these potential issues with absolute thresholds, they have been applied with good results in some centers—most notably for core CBV assessment.<sup>48-51</sup> Receiver operating characteristic curve analysis in 130 patients suspected of having acute ischemic stroke suggested that relative MTT was the CTP parameter most accurately characterizing salvageable penumbra, and absolute CBV, the parameter most accurately characterizing infarct core at admission, again with an optimal threshold of 2.0 mL/100 g.<sup>47</sup>

An additional alternative approach for determining threshold values for penumbra and core in gray matter<sup>52</sup> differs from that in previous work because it incorporates the

interaction between CBF and CBV. Logistic regression was applied to data points from patients who underwent recanalization of occluded vessels to define thresholds for separating core from penumbra. Because infarct CBF is slightly lower and CBV much lower than that in penumbral tissue, the separation between infarct and penumbra was maximized when a threshold based on the product of 2 values (CBF × CBV) was used as a discriminator. CBF × CBV resulted in a significantly better separation between infarct and penumbra than CBF or CBV alone, suggesting that the CBV threshold for infarction varies with CBF. Future prospective studies will determine the clinical utility of this approach. The same research group has applied this methodology to white matter with equally good separation between infarct and penumbra.<sup>53</sup>

**The Best Possible Perfusion Parameter to Define Salvageable Penumbra?** Whereas calculation of CBV, CBF, and MTT requires off-line processing, typically with deconvolution, other parameters may require less complex data processing, and, with MRP especially, are often immediately accessible at the scanner. Time to peak (TTP) provides a measurement of transit time, as its name suggests, and is calculated with a straightforward analysis of the TDC. Lengthening of the time required for the passage of a contrast bolus through the brain, with prolongation of MTT and TTP, is a common finding in ischemic tissue. MTT and TTP prolongation, however, may also be false-positive for ischemia, with oligemia and hypoperfusion, but not true hypoxia, in the setting of a severe extracranial carotid stenosis/occlusion or delayed intracranial flow due to atrial fibrillation or low ejection fraction.<sup>54,55</sup>

To date, different perfusion parameters with different thresholds have been applied for penumbral assessment in different centers, potentially resulting in different estimates of abnormal perfusion and different patient management decisions. This variability needs to be addressed in definitive trials, with validation of optimal postprocessing and image interpretation procedures, followed by standardization of methodology across different centers.

To date, published studies investigating the various perfusion maps have drawn sometimes different conclusions regarding the optimal admission penumbral parameter for predicting outcome. Two MRP studies have reported that TTP is correlated with baseline NIH Stroke Scale (NIHSS) score,<sup>56,57</sup> one has suggested a correlation between MTT and the Scandinavian Stroke Scale score,<sup>58</sup> 2 have reported a correlation between MTT and NIHSS score,<sup>59,60</sup> and 3 have reported correlations between MTT and 60- or 90-day follow-up T2 lesions.<sup>56,57,61</sup> A recent report by Kane et al (2007)<sup>62</sup> addressed this issue by comparing 10 different MRP processing methods in 32 patients with acute ischemic stroke. Different perfusion parameters produced very different estimates of abnormal perfusion in the same data from the same patients, and, therefore, different estimates of penumbral volume. All 5 measures of MTT were associated with baseline NIHSS score and final infarct size; 1 of the MTT measures was fitted arrival time, which was also associated with clinical outcome. Validation of these findings in other datasets is sorely needed so that consensus can be reached regarding which perfusion measures and processing methods should be used routinely.

Finally, with regard to display of CTP images, the ASIST

group from Japan has advocated replacement of operator-dependent color-scale adjustment with automated color-scale display, to minimize variations in the visual interpretation of perfusion maps.

### Clinical Implications

The ability of perfusion imaging to discriminate between ischemic core and penumbra is important in ongoing and future clinical trials. There is currently good level II evidence suggesting that core/penumbra mismatch will be important for patient selection for stroke recanalization therapies extending beyond the current arbitrary cutoffs of 3 hours postictus for intravenous thrombolysis and 6 hours postictus for intra-arterial thrombolysis.<sup>63-66</sup> This review has summarized the pearls and pitfalls of CTP theory, acquisition, postprocessing, and image interpretation.

Optimal acquisition requires scanning for at least 60–75 seconds and strategies for maximizing z-dimension coverage. The addition of a cardiac MDCT component to assess cardioembolic sources of stroke is an appealing addition to the current integrated neurovascular protocol comprising unenhanced CT, CTA, and CTP.

Optimal postprocessing might be achieved with nonparametric deconvolution techniques, such as SVD. Vascular pixel elimination and bolus-tracer delay correction with 1 of the several available methods will likely prove essential for postprocessing optimization, whereas the laterality of AIF selection is unlikely to be an important consideration, with the more widespread application of delay-corrected postprocessing software.

Optimal image interpretation requires selection of appropriate CBV and CBF thresholds and choice of the most appropriate perfusion parameter for an operational definition of penumbra. This is a controversial topic; though recent studies have suggested that arrival-time-fitted MTT maps are well correlated with clinical and radiologic outcomes, much work remains to be done so that perfusion imaging is “ready for prime time.”<sup>62</sup> Whether relative or absolute CTP thresholds for core and penumbra are optimal and the degree to which this distinction matters also remain an open question.

Validation and standardization of CTP methodology will be crucial for the widespread acceptance of advanced imaging in patient selection for novel stroke therapies. Expert consensus regarding standardization of CTP image acquisition has already been reached at the Advanced Neuroimaging for Acute Stroke Treatment meeting held in the fall of 2007 in Washington, DC.<sup>2,3</sup> Both this group and the ASIST group in Japan, however, have emphasized the continued need for definitive optimization and validation of commercially available CTP postprocessing software, especially with regard to the necessity for deconvolution methods and delay correction.

Once validation is achieved, standardization will minimize interobserver and interhospital variability in selecting patients for novel therapies, including thrombolysis beyond the currently accepted time windows. Level I evidence of improvement in patient outcome by using advanced perfusion imaging is of course the ultimate goal. Standardization of CTP acquisition, postprocessing, and interpretation techniques will likely facilitate future randomized controlled trials that will provide the level I evidence that CTP mismatch is of value

in patient selection for the next generation of novel stroke therapies.

### References

1. Konstas AA, Goldmakher GV, Lee T-Y, et al. **Theoretic basis and technical implementations of CT perfusion in acute ischemic stroke, Part 1. Theoretic basis.** *AJNR Am J Neuroradiol* 2009;30:662–68
2. Wintermark M, Albers GW, Alexandrov AV, et al. **Acute stroke imaging research roadmap.** *AJNR Am J Neuroradiol* 2008;29:e23–30
3. Wintermark M, Albers GW, Alexandrov AV, et al. **Acute stroke imaging research roadmap.** *Stroke* 2008;39:1621–28
4. Shetty SK, Lev MH. **CT perfusion in acute stroke.** *Neuroimaging Clin N Am* 2005;15:481–501
5. White H, Boden-Albala B, Wang C, et al. **Ischemic stroke subtype incidence among whites, blacks, and Hispanics: the Northern Manhattan Study.** *Circulation* 2005;111:1327–31
6. Shapiro MD, Neilan TG, Jassal DS, et al. **Multidetector computed tomography for the detection of left atrial appendage thrombus: a comparative study with transesophageal echocardiography.** *J Comput Assist Tomogr* 2007;31:905–09
7. Kim YY, Klein AL, Halliburton SS, et al. **Left atrial appendage filling defects identified by multidetector computed tomography in patients undergoing radiofrequency pulmonary vein antral isolation: a comparison with transesophageal echocardiography.** *Am Heart J* 2007;154:1199–205
8. Cenic A, Nabavi DG, Craen RA, et al. **Dynamic CT measurement of cerebral blood flow: a validation study.** *AJNR Am J Neuroradiol* 1999;20:63–73
9. Nabavi DG, Cenic A, Craen RA, et al. **CT assessment of cerebral perfusion: experimental validation and initial clinical experience.** *Radiology* 1999;213:141–49
10. Miles KA. **Perfusion CT for the assessment of tumour vascularity: which protocol?** *Br J Radiol* 2003;76 (Spec No 1):S36–42
11. Lorberboym M, Lampl Y, Sadeh M. **Correlation of 99mTc-DTPA SPECT of the blood-brain barrier with neurologic outcome after acute stroke.** *J Nucl Med* 2003;44:1898–904
12. Kassner A, Roberts T, Taylor K, et al. **Prediction of hemorrhage in acute ischemic stroke using permeability MR imaging.** *AJNR Am J Neuroradiol* 2005;26:2213–17
13. Lee TY. **Scientific basis and validation.** In: Miles KA, Eastwood JD, Konig M, eds. *Multidetector Computed Tomography in Cerebrovascular Disease: CT Perfusion Imaging.* Abingdon, UK: Informa Healthcare; 2007:13–27
14. Lee TY, Stewart E. **Scientific basis and validation.** In: Miles KA, Charnsangavej C, Cuenod CA, eds. *Multidetector Computed Tomography in Oncology: CT Perfusion Imaging.* Abingdon, UK: Informa Healthcare; 2007
15. Nabavi DG, Cenic A, Dool J, et al. **Quantitative assessment of cerebral hemodynamics using CT: stability, accuracy, and precision studies in dogs.** *J Comput Assist Tomogr* 1999;23:506–15
16. Wintermark M, Maeder P, Verdun FR, et al. **Using 80 kVp versus 120 kVp in perfusion CT measurement of regional cerebral blood flow.** *AJNR Am J Neuroradiol* 2000;21:1881–84
17. Roberts HC, Roberts TP, Smith WS, et al. **Multisection dynamic CT perfusion for acute cerebral ischemia: the “toggling-table” technique.** *AJNR Am J Neuroradiol* 2001;22:1077–80
18. Wintermark M, Reichhart M, Thiran JP, et al. **Prognostic accuracy of cerebral blood flow measurement by perfusion computed tomography, at the time of emergency room admission, in acute stroke patients.** *Ann Neurol* 2002;51:417–32
19. Wintermark M, Smith WS, Ko NU, et al. **Dynamic perfusion CT: optimizing the temporal resolution and contrast volume for calculation of perfusion CT parameters in stroke patients.** *AJNR Am J Neuroradiol* 2004;25:720–29
20. Smith AB, Dillon WP, Gould R, et al. **Radiation dose-reduction strategies for neuroradiology CT protocols.** *AJNR Am J Neuroradiol* 2007;28:1628–32
21. Hamberg LM, Rhea JT, Hunter GJ, et al. **Multi-detector row CT: radiation dose characteristics.** *Radiology* 2003;226:762–72
22. Lee TYM B, Chen X, Miles KA. **Image processing.** In: Miles KA, Eastwood JD, Konig M, eds. *Multidetector Computed Tomography in Cerebrovascular Disease: CT Perfusion Imaging.* Abingdon, UK: Informa Healthcare; 2007:57–69
23. Sanelli PC, Lev MH, Eastwood JD, et al. **The effect of varying user-selected input parameters on quantitative values in CT perfusion maps.** *Acad Radiol* 2004;11:1085–92
24. Kudo K, Terae S, Katoh C, et al. **Quantitative cerebral blood flow measurement with dynamic perfusion CT using the vascular-pixel elimination method: comparison with H<sub>2</sub>(15)O positron emission tomography.** *AJNR Am J Neuroradiol* 2003;24:419–26
25. Calamante F, Gadian DG, Connelly A. **Delay and dispersion effects in dynamic susceptibility contrast MRI: simulations using singular value decomposition.** *Magn Reson Med* 2000;44:466–73
26. Calamante F, Yim PJ, Cebra JR. **Estimation of bolus dispersion effects in perfusion MRI using image-based computational fluid dynamics.** *Neuroimaging* 2003;19:341–53
27. Wu O, Ostergaard L, Weisskoff RM, et al. **Tracer arrival timing-insensitive**

- technique for estimating flow in MR perfusion-weighted imaging using singular value decomposition with a block-circulant deconvolution matrix. *Magn Reson Med* 2003;50:164–74
28. Wittsack HJ, Wohlschlagel AM, Ritzl EK, et al. CT-perfusion imaging of the human brain: advanced deconvolution analysis using circulant singular value decomposition. *Comput Med Imaging Graph* 2008;32:67–77
  29. van Osch MJ, Vonken EJ, Bakker CJ, et al. Correcting partial volume artifacts of the arterial input function in quantitative cerebral perfusion MRI. *Magn Reson Med* 2001;45:477–85
  30. Lin W, Celik A, Derdeyn C, et al. Quantitative measurements of cerebral blood flow in patients with unilateral carotid artery occlusion: a PET and MR study. *J Magn Reson Imaging* 2001;14:659–67
  31. Lorenz C, Benner T, Chen PJ, et al. Automated perfusion-weighted MRI using localized arterial input functions. *J Magn Reson Imaging* 2006;24:1133–39
  32. Mouridsen K, Christensen S, Gyldensted L, et al. Automatic selection of arterial input function using cluster analysis. *Magn Reson Med* 2006;55:524–31
  33. Calamante F, Morup M, Hansen LK. Defining a local arterial input function for perfusion MRI using independent component analysis. *Magn Reson Med* 2004;52:789–97
  34. Ibaraki M, Shimosegawa E, Toyoshima H, et al. Tracer delay correction of cerebral blood flow with dynamic susceptibility contrast-enhanced MRI. *J Cereb Blood Flow Metab* 2005;25:378–90
  35. Mui K, Nogueira R, Lev MH, et al. CT CBV lesions do not always infarct in acute stroke following IA and IV thrombolysis: In: *Proceedings of the 46th Annual Meeting of the American Society of Neuroradiology, New Orleans, La, June 2, 2008*
  36. Bisdas S, Konstantinou GN, Gurung J, et al. Effect of the arterial input function on the measured perfusion values and infarct volumetric in acute cerebral ischemia evaluated by perfusion computed tomography. *Invest Radiol* 2007;42:147–56
  37. Thijs VN, Adami A, Neumann-Haefelin T, et al. Relationship between severity of MR perfusion deficit and DWI lesion evolution. *Neurology* 2001;57:1205–11
  38. Rose SE, Janke AL, Griffin M, et al. Improving the prediction of final infarct size in acute stroke with bolus delay-corrected perfusion MRI measures. *J Magn Reson Imaging* 2004;20:941–47
  39. Goldmakher GV, Kamalian S, Schaefer PW, et al. Fully automated processing of stroke CT perfusion maps is fast and accurate. In: *Radiological Society of North America Scientific Assembly and Annual Meeting Program*. Oak Brook, Ill: November 29, 2006
  40. Fiorella D, Heiserman J, Prenger E, et al. Assessment of the reproducibility of postprocessing dynamic CT perfusion data. *AJNR Am J Neuroradiol* 2004;25:97–107
  41. Warach S. Measurement of the ischemic penumbra with MRI: it's about time. *Stroke* 2003;34:2533–34
  42. Wu O, Koroshetz WJ, Ostergaard L, et al. Predicting tissue outcome in acute human cerebral ischemia using combined diffusion- and perfusion-weighted MR imaging. *Stroke* 2001;32:933–42
  43. Barber PA, Darby DG, Desmond PM, et al. Prediction of stroke outcome with echoplanar perfusion- and diffusion-weighted MRI. *Neurology* 1998;51:418–26
  44. Koenig M, Kraus M, Theek C, et al. Quantitative assessment of the ischemic brain by means of perfusion-related parameters derived from perfusion CT. *Stroke* 2001;32:431–37
  45. Powers WJ, Grubb RL Jr, Raichle ME. Physiological responses to focal cerebral ischemia in humans. *Ann Neurol* 1984;16:546–52
  46. Schaefer PW, Roccatagliata L, Ledezma C, et al. First-pass quantitative CT perfusion identifies thresholds for salvageable penumbra in acute stroke patients treated with intra-arterial therapy. *AJNR Am J Neuroradiol* 2006;27:20–25
  47. Wintermark M, Flanders AE, Velthuis B, et al. Perfusion-CT assessment of infarct core and penumbra: receiver operating characteristic curve analysis in 130 patients suspected of acute hemispheric stroke. *Stroke* 2006;37:979–85
  48. Hossmann KA. Viability thresholds and the penumbra of focal ischemia. *Ann Neurol* 1994;36:557–65
  49. Harper AM. Autoregulation of cerebral blood flow: influence of the arterial blood pressure on the blood flow through the cerebral cortex. *J Neurol Neurosurg Psychiatry* 1966;29:398–403
  50. Lee KH, Cho SJ, Byun HS, et al. Triphasic perfusion computed tomography in acute middle cerebral artery stroke: a correlation with angiographic findings. *Arch Neurol* 2000;57:990–99
  51. Mayer TE, Hamann GF, Baranczyk J, et al. Dynamic CT perfusion imaging of acute stroke. *AJNR Am J Neuroradiol* 2000;21:1441–49
  52. Murphy BD, Fox AJ, Lee DH, et al. Identification of penumbra and infarct in acute ischemic stroke using computed tomography perfusion-derived blood flow and blood volume measurements. *Stroke* 2006;37:1771–77
  53. Murphy BD, Fox AJ, Lee DH, et al. White matter thresholds for the ischemic penumbra and infarct core in patients with acute stroke: CT perfusion study. *Radiology* 2008;247:818–25. Epub 2008 Apr 18
  54. Eastwood JD, Lev MH, Azhari T, et al. CT perfusion scanning with deconvolution analysis: pilot study in patients with acute middle cerebral artery stroke. *Radiology* 2002;222:227–36
  55. Sorensen A, Copen W, Ostergaard L, et al. Hyperacute stroke: simultaneous measurement of relative cerebral blood volume, relative cerebral blood flow and mean tissue transit time. *Radiology* 1999;210:519–27
  56. Beaulieu C, de Crespigny A, Tong DC, et al. Longitudinal magnetic resonance imaging study of perfusion and diffusion in stroke: evolution of lesion volume and correlation with clinical outcome. *Ann Neurol* 1999;46:568–78
  57. Derex L, Nighoghossian N, Hermier M, et al. Influence of pretreatment MRI parameters on clinical outcome, recanalization and infarct size in 49 stroke patients treated by intravenous tissue plasminogen activator. *J Neurol Sci* 2004;225:3–9
  58. Rohl L, Geday J, Ostergaard L, et al. Correlation between diffusion- and perfusion-weighted MRI and neurological deficit measured by the Scandinavian Stroke Scale and Barthel Index in hyperacute subcortical stroke ( $\leq 6$  hours). *Cerebrovasc Dis* 2001;12:203–13
  59. Parsons MW, Barber PA, Chalk J, et al. Diffusion- and perfusion-weighted MRI response to thrombolysis in stroke. *Ann Neurol* 2002;51:28–37
  60. Barber PA, Parsons MW, Desmond PM, et al. The use of PWI and DWI measures in the design of “proof-of-concept” stroke trials. *J Neuroimaging* 2004;14:123–32
  61. Butcher K, Parsons M, Baird T, et al. Perfusion thresholds in acute stroke thrombolysis. *Stroke* 2003;34:2159–64
  62. Kane I, Carpenter T, Chappell F, et al. Comparison of 10 different magnetic resonance perfusion imaging processing methods in acute ischemic stroke: effect on lesion size, proportion of patients with diffusion/perfusion mismatch, clinical scores, and radiologic outcomes. *Stroke* 2007;38:3158–64
  63. Hacke W, Albers G, Al-Rawi Y, et al. The Desmoteplase in Acute Ischemic Stroke Trial (DIAS): a phase II MRI-based 9-hour window acute stroke thrombolysis trial with intravenous desmoteplase. *Stroke* 2005;36:66–73
  64. Albers GW. Expanding the window for thrombolytic therapy in acute stroke: the potential role of acute MRI for patient selection. *Stroke* 1999;30:2230–37
  65. Muir KW, Grosset DG. Neuroprotection for acute stroke: making clinical trials work. *Stroke* 1999;30:180–82
  66. Furlan AJ, Eyding D, Albers GW, et al. Dose Escalation of Desmoteplase for Acute Ischemic Stroke (DEDAS): evidence of safety and efficacy 3 to 9 hours after stroke onset. *Stroke* 2006;37:1227–31